AD-A100 911 COLORADO UNIV AT BOULDER DEPT OF ELECTRICAL ENGINEERING F/G 7/2
PROPERTIES AND APPLICATIONS OF GAINASP.(U)
MAR 81 R E HAYES N00014-75-C-0472
UNCLASSIFIED NL

1 OF 1
AD A
100911

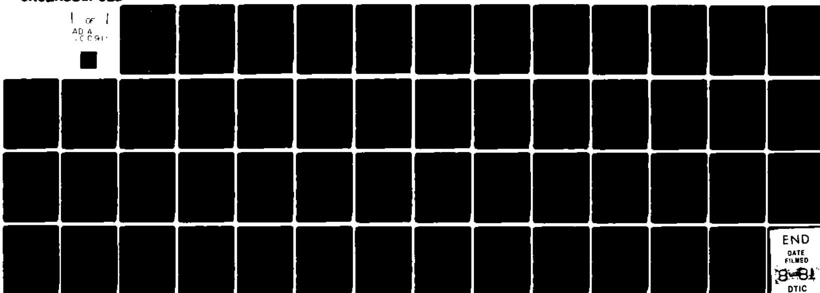

END
DATE FILMED
8-81
DTIC

LEVEL II

(12)

PROPERTIES AND APPLICATIONS OF GaInAsP

Final Report

ONR Contract N00014-75-C-0472

DTIC FILE COPY

Russell E. Hayes
Principal Investigator

March 20, 1981

11 Mar 81 12 32

Department of Electrical Engineering
University of Colorado
Boulder, Colorado 80309

DISTRIBUTION STATEMENT A
Approved for public release;
Distribution Unlimited

81 3 24 086

ABSTRACT

This research program, supported by ONR Contract N00014-75-C-0472, involved the investigation of several aspects of $Ga_xIn_{1-x}As_yP_{1-y}$, grown by LPE, that are of importance to the potential use of this material for field effect transistors, transferred-electron oscillators, and other devices. Results obtained include: various electrical characteristics of the material; the observation that the GaInAsP-InP conduction band discontinuity was less than 60 meV for these junctions; the characteristics of some quaternary transferred electron oscillators; and the properties of anodic oxides grown on the quaternary.

Accession For
NTIS GRA&I
DTIC TAB
Unannounced
Justification
By
Distribution/
Availability Codes
Avail and/or
Dist Special
A

CONTENTS

PAGE

ABSTRACT - 2

1. INTRODUCTION - 4

2. LIQUID-PHASE EPITAXIAL GROWTH - - - - - - - - - - - - - - - 6

2.1 Surface Morphology and Epi-Layer Thickness - - - - 6

2.2 Lattice Constant and Energy Bandgap Results - - - 7

2.3 Surface Compositional Homogeneity - - - - - - - - 7

3. ELECTRICAL PROPERTIES - - - - - - - - - - - - - - - - - 15

3.1 Experimental Results - - - - - - - - - - - - - - - 15

3.2 Calculated Mobility - - - - - - - - - - - - - - - - 16

4. HETEROJUNCTION STUDIES - - - - - - - - - - - - - - - - - 22

4.1 Experimental Heterojunction Diodes - - - - - - - - - 22

4.2 Interpretation of the Data - - - - - - - - - - - - - 27

5. TRANSFERRED ELECTRON EFFECT - - - - - - - - - - - - - - - 30

6. ANODIC OXIDES - 31

6.1 MOS Measurements - - - - - - - - - - - - - - - - - - 31

6.2 Surface-State Time Constants - - - - - - - - - - - - - 34

7. CONCLUSION - 45

8. REFERENCES - 47

APPENDIX 1 - 50

1. INTRODUCTION

This is a final summary technical report which outlines research on the properties and device aspects of the quaternary semiconductor compound $Ga_xIn_{1-x}As_yP_{1-y}$. The work described here was supported by the Office of Naval Research through ONR Contract N00014-75-C-0472, during the period 2-1-74 through 10-31-79.

The principal topics concerning GaInAsP that are summarized in this report include the liquid phase epitaxy of the material, the observed electrical properties, characteristics of n-n heterojunction diodes, the transferred-electron effect, and the properties of anodic oxides produced on the quaternary.

Detailed technical reports dealing with the topics discussed here are available from R.E. Hayes, Electrical Engineering Department, University of Colorado, Boulder, Colorado 80309. These seven technical reports are:

"Growth and Characterization of $In_xGa_{1-x}As_yP_{1-y}$-InP n-n Heterojunctions," S.C. Wright, Solid State Electronics Report 78-5-1.

"An Electrical Evaluation of $Ga_xIa_{1-x}As_yP_{1-y}$", E.F. Marchand, Solid State Electronics Report 79-6-1.

"Characteristics of Anodic Oxide Films on InP and GaInAsP", A.A.R. Elshabini, Solid State Electronics Report 78-5-2.

"A Study of Surface State Parameters and an Investigation of the Surface Charge Behavior with Charging Frequency for InP and $In_xGa_{1-x}As_yP_{1-y}$ Materials", M.M. El-Muradi, Solid State Electronics Report 79-4-1.

"Mobility and Carrier Concentration in GaAs and GaInAsP", C.D. Forgerson, Solid State Electronics Report 81-3-1.

"Tables of the Compositional Dependence of the Energy Bandgap and Lattice Constant for $Ga_xIn_{1-x}As_yP_{1-y}$", R.E. Hayes, Solid State Electronics Report 77-6-1.

"Tables of LPE Composition Parameters for Ga InAsP", R.E. Hayes, Solid State Electronics Report 78-7-1.

2. LIQUID-PHASE EPITAXIAL GROWTH

The $Ga_xIn_{1-x}As_yP_{1-y}$ layers investigated were grown on InP substrates by liquid-phase epitaxy (LPE) using the so-called sliding boat technique with ramp cooling of a single-phase melt that had been previously saturated with P from an InP source. Substrate preparation and related techniques are given in Appendix 1. A discussion of the growth system used is given in a Technical Report [1].

The Ga-In-As-P melt compositions for growth starting at approximately 650°C were determined by using published Ga and As distribution coefficients as a guideline and then empirically determining the melt composition that gives a lattice-matched epitaxial layer. The lattice constant and bandgap of the epitaxial layers were determined by X-ray diffraction and photoluminescence respectively.

2.1 Surface Morphology and Epi-Layer Thickness

A wide variety of surface features appeared for lattice-matched compositions. Although the detailed morphology varied considerably between epi-layers, a number of features were commonly observed. These included waves or steps, probably due to substrate orientation, meniscus lines, and pits due to out diffusion of phosphorous from the substrate. The best layers were quite smooth with a mirror surface. The over-all epi-layer thickness variations were significant, both between repeated growths (under identical conditions) as

well as from point to point in a single epi-layer. Thickness variation across a typical layer was as much as 30%. An average epi-layer thickness for a 20 minute growth time (650-630°C ramp cooling) was about 5 microns. This yields an average growth rate of approximately 0.25 microns/min. Figure 2.1 shows a photograph taken through an optical microscope of cleaved and stained edges of an epitaxial quaternary layer. The epitaxial layer was delineated using A-B etch (Appendix 1).

2.2 Lattice Constant and Energy Bandgap Results

The energy bandgap of each epi-layer was determined by a photoluminescence measurement using an Argon laser (or high-intensity Hg arc lamp) and a 0.6 meter focal length spectrometer. The luminescence spectrum peak was used to determine the bandgap although this gives a slight error.

The lattice constant was determined for a number of epi-layers from X-ray diffraction data. This data, together with Auger spectroscopy data to determine composition served as checks on the melt constituent calculations. The bandgap and lattice constant were related to the semiconductor composition through empirical relations described in a Technical Report [2]. Figure 2.2 shows a typical photoluminescence result and Figures 2.3 and 2.4 are graphical presentations of selected lattice constant and energy bandgap data.

2.3 Surface Compositional Homogeneity

To study the homogeneity of the epi-layer composition across the surface, an electron microprobe analysis was performed

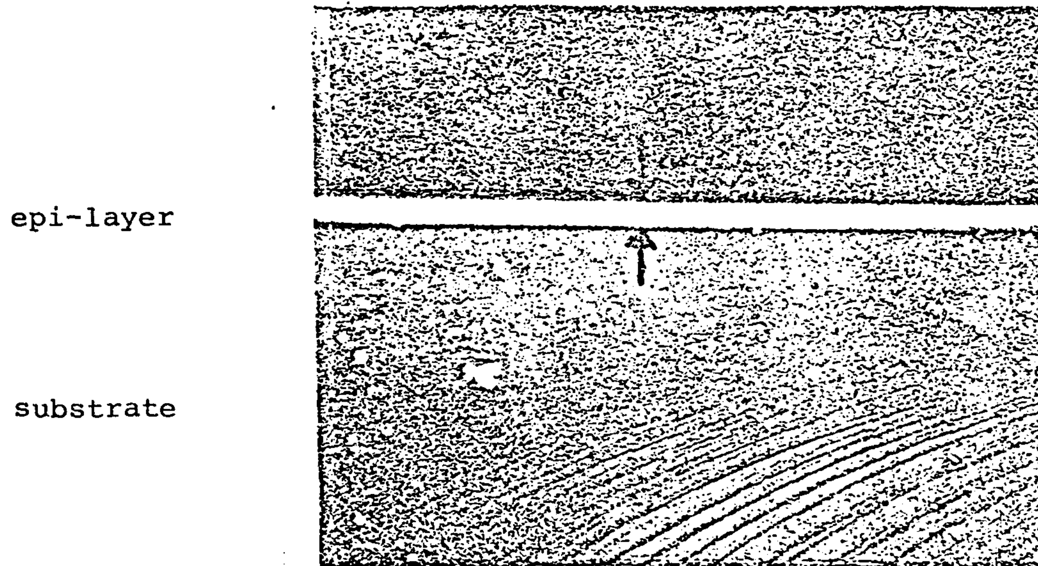

Fig. 2.1 Photograph of epitaxial layer Cl-028 (450x). The layer is approximately 4.5 μm thick.

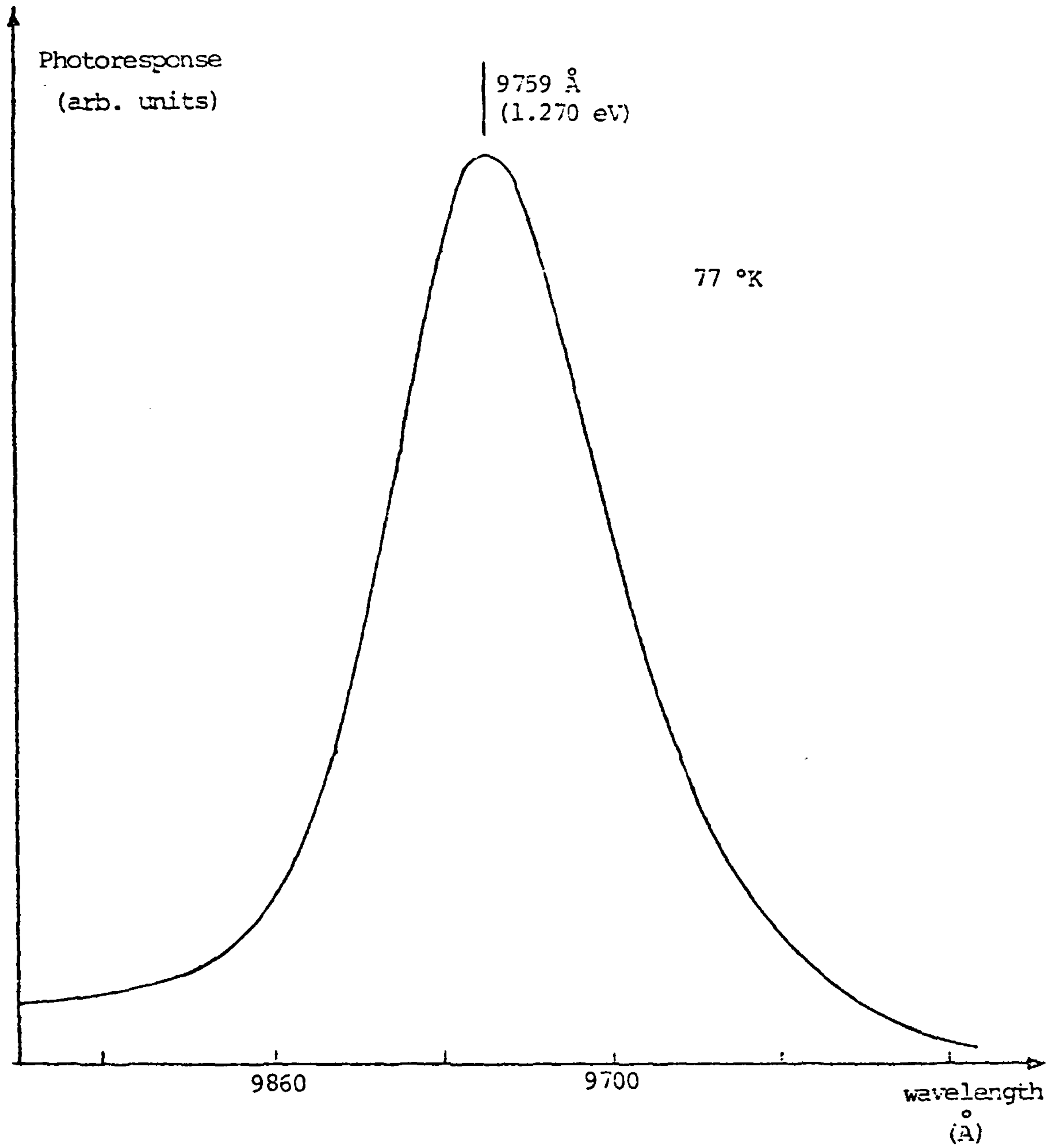

Fig. 2.2 Photoluminescence Spectral Response (Cl-029)

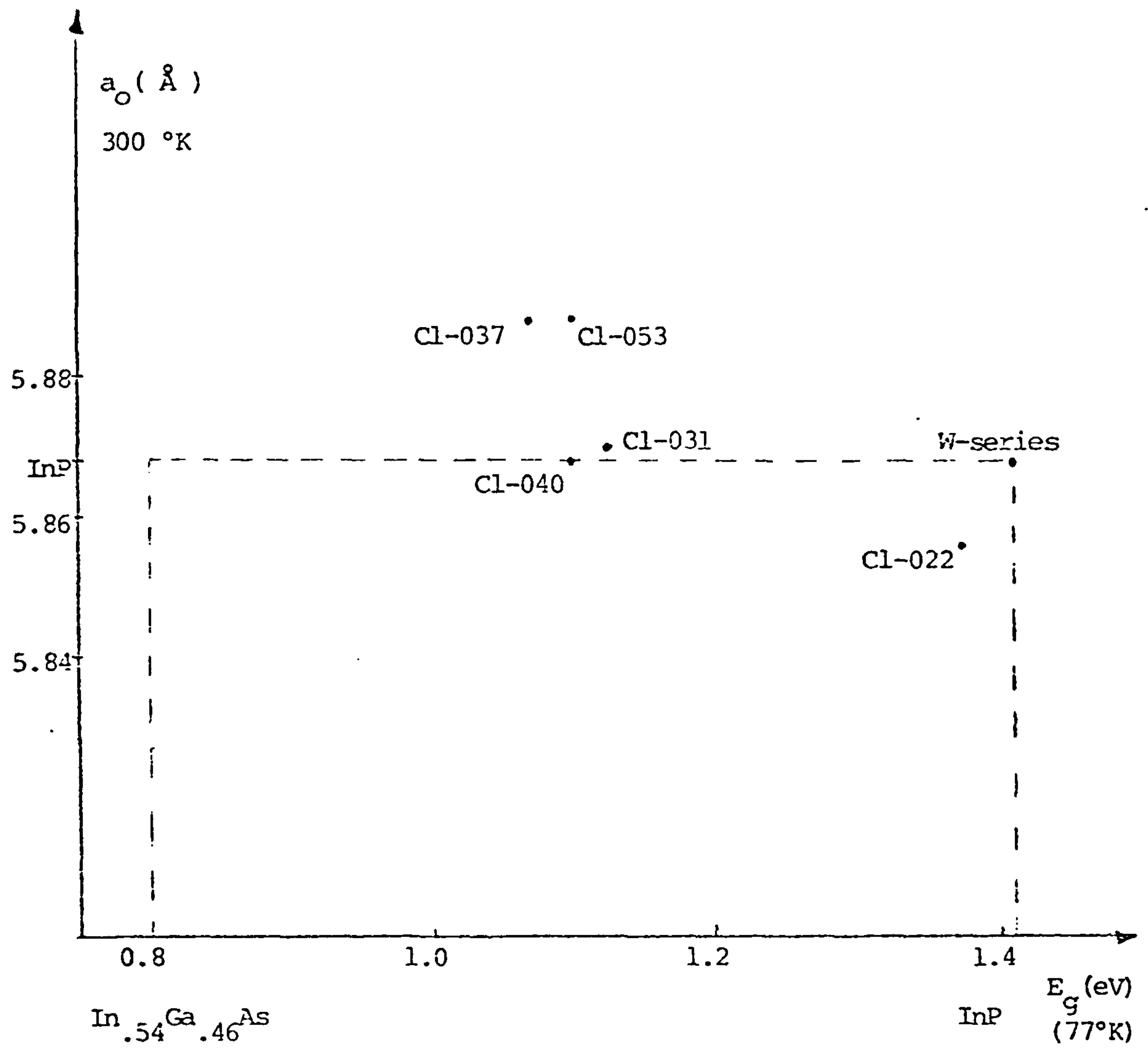

Fig. 2.3 Selected Lattice Constant and Energy Bandgap Data of Various Epi-layers.

The lattice constants were determined from X-ray diffraction and the energy bandgap from photoluminescence experiments.

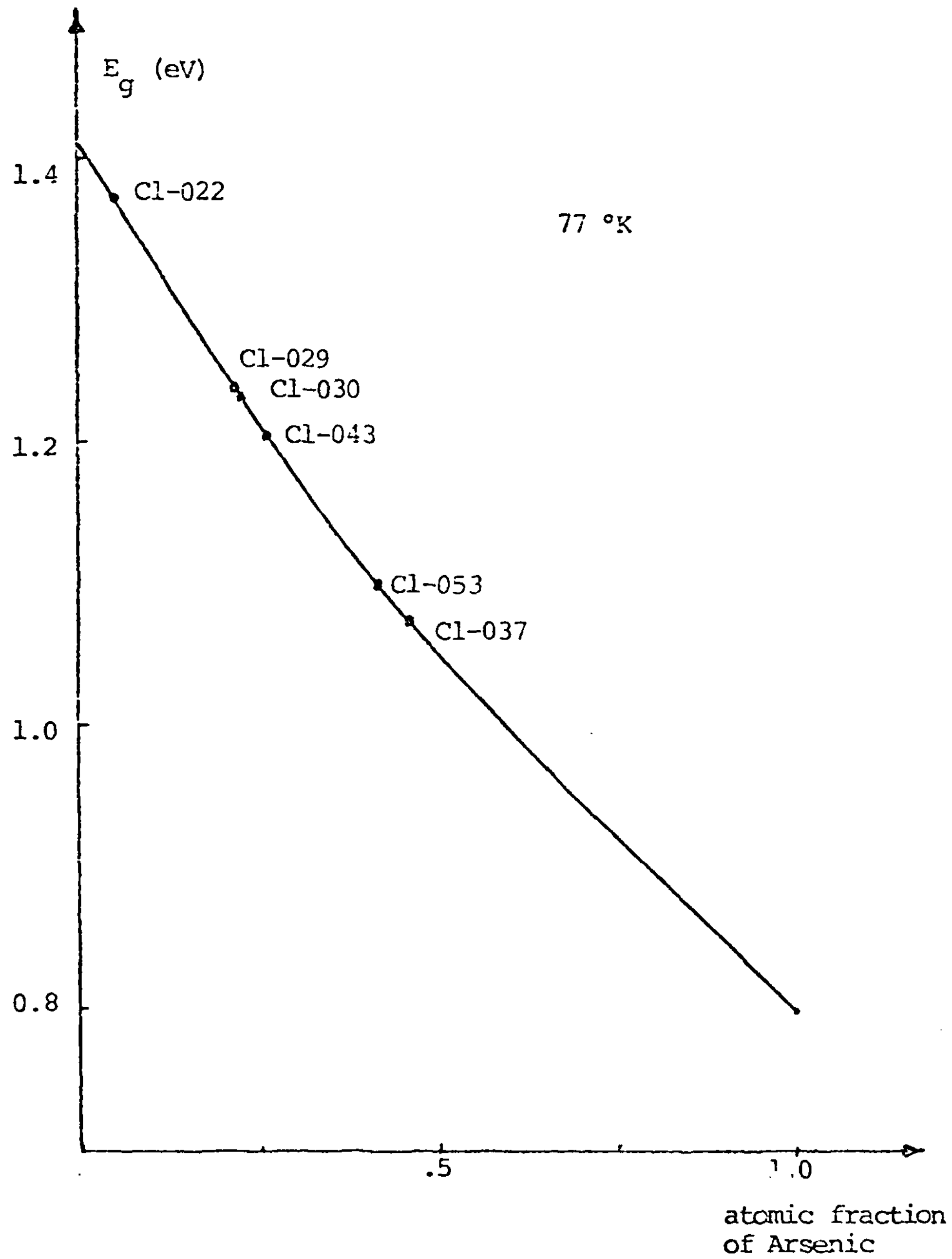

Fig. 2.4 Energy Bandgap vs. Arsenic Concentration

This is a plot of the energy bandgaps of various epi-layers vs. the theoretical Arsenic concentration as determined from the empirical equations discussed in section 1.5.

on sample Cl-065. The two standards which were used were GaAs and InP, each of which has a rigid stoichiometry of fifty atomic percent for each element.

At eight locations on the surface, two sets of X-ray counts were taken. The beam spots for the two sets were focused within 50 microns of each other at each location. In computer analysis of the data, comparison with the known standards does not assure one-to-one stoichiometry between group III and group V elements. This means that the absolute accuracy of the atomic fraction of each element is in doubt. However, accuracy of each surface measurement relative to one another is still quite high. The standard deviation in the atomic fraction of each element was found to be less than or equal to one percent. Figure 2.5 is a table summarizing the results.

The predicted values were determined from the known melt composition and experimentally determined distribution coefficients. The average values and standard deviations were determined from the eight sets of surface measurements. Since the sum of the atomic percentages of the group III (or group V) elements is roughly 2.5% off from the ideal 50% value, the absolute accuracy of each average value is at best a few percent.

It should be noted that the x and y values ($Ga_xIn_{1-x}As_yP_{1-y}$) determined from the Cl-065 data given in Fig. 2.5 are $x = 0.08$ and $y = 0.42$. These results are in reasonable agreement with the lattice-match conditions determined from empirical data on ternaries and described in a technical

Element	Predicted Values (atomic %)	Microprobe Results average (atomic %)	standard deviation (atomic %)
Ga	12	10.2	0.34
In	38	37.3	1.15
As	21	24.4	0.95
P	29	28.1	0.47

Fig. 2.5 Surface Composition Data

report giving the relation between composition, bandgap, and lattice constant of the quaternary [2].

3. ELECTRICAL PROPERTIES

This section contains a summary of the carrier density and mobility characteristics of the quaternary epitaxial layers that were investigated, and an evaluation of the scattering mechanisms that lead to the observed mobility. Two technical reports that cover the details of these investigations of electrical properties are available [3,4].

3.1 Experimental Results

The quaternary layers that have been studied were n-type, not intentionally doped, usually having electron densities in the 10^{16} cm^{-3} range. Four-point probe measurements of quaternary epitaxial layers grown on high resistivity substrates indicated that the layer resistivity varied by about $\pm 10\%$ over the surface. Thus it appears reasonable to assume that the layer properties were essentially uniform over the surface.

Electron mobility and concentration were measured as a function of temperature by the van der Pauw technique in order to establish the layer compensation and identify the presence of any deep energy levels. Epitaxial layers for this purpose were typically 2.5 μm thick grown on (100) oriented Fe doped InP substrates ($\rho > 10^8$ Ω-cm). The ohmic contacts to the edge of the epitaxial layer were 6-9's pure In hemispheres about 0.7 mm in diameter that were pressed into place. These contacts were observed to be ohmic at the current and temperature values used in the measurements. Typical results are shown in

Figures 3.1 and 3.2. Note that the scattering correction factor relating the Hall and drift mobilities, r, has been taken as unity in this report. Theoretical calculations taking the various scattering mechanisms into account indicate that r varies over the range 1.21-1.27 for the temperatures shown in the figures [3]. These typical experimental mobility results are interpreted in Section 3.2 in terms of a compensation ratio N_A/N_D of about 0.7.

3.2 Calculated Mobility

The variation of electron mobility with temperature was studied in order to identify the principle scattering mechanisms involved. Theoretical calculations based on previous work were used to determine the expected quaternary mobility characteristics [3,4]. There are three primary scattering mechanisms which determine the mobility of GaInAsP. They are polar optical phonon scattering, acoustic deformation potential scattering, and ionized impurity scattering. Calculated contributions from alloy scattering were small and are not included in the results described here.

Polar optical scattering was calculated following Harrison & Hauser as well as others [5,3,6]. The ionized impurity scattering calculation was based on the work of Brooks and Herring as described in the references [3,4]. Acoustic phonon deformation potential scattering was based on results given by Nag [7]. The quaternary parameters needed in the scattering calculations were obtained from binary parameters using

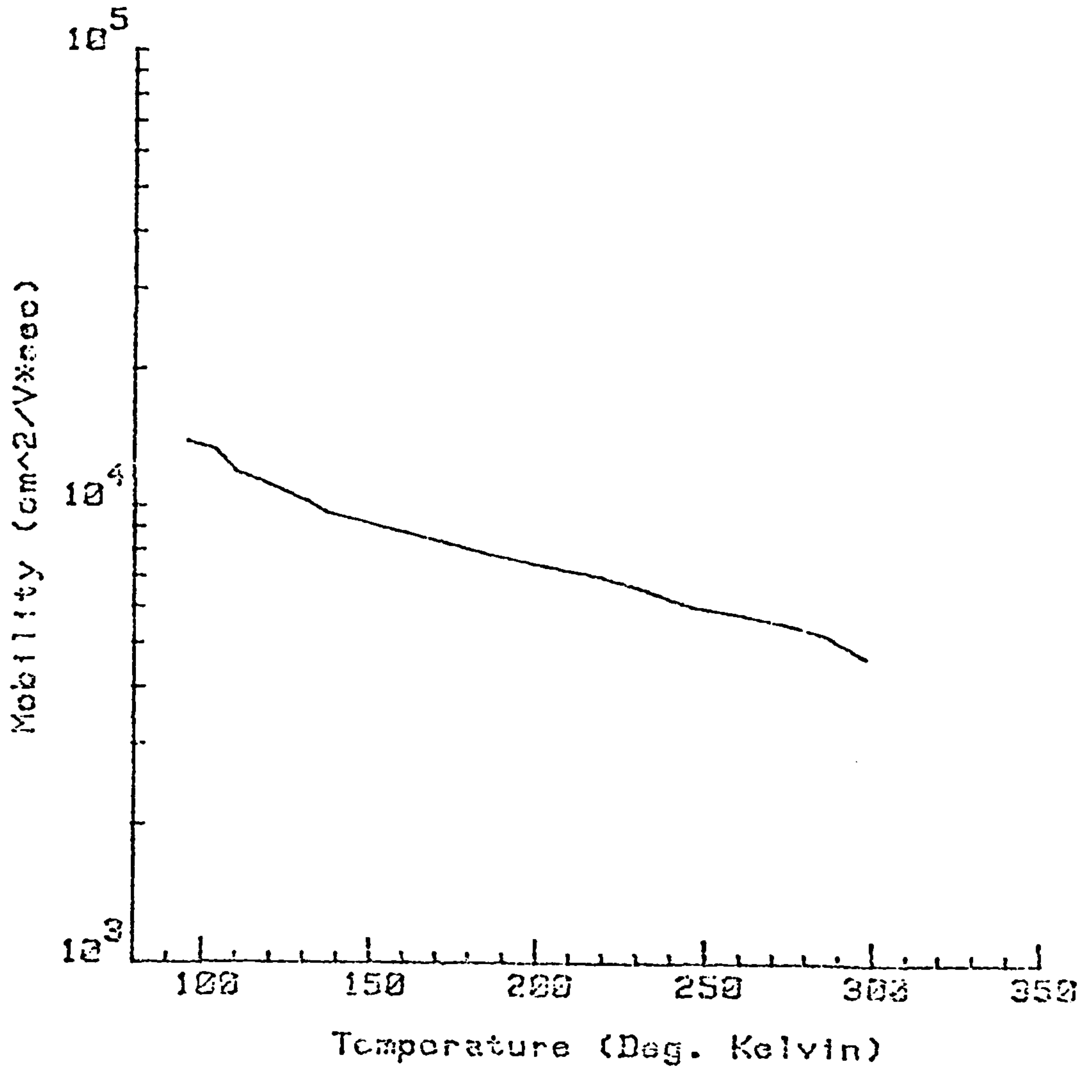

Fig. 3.1 Mobility versus temperature -- GaInAsP sample C1-121.

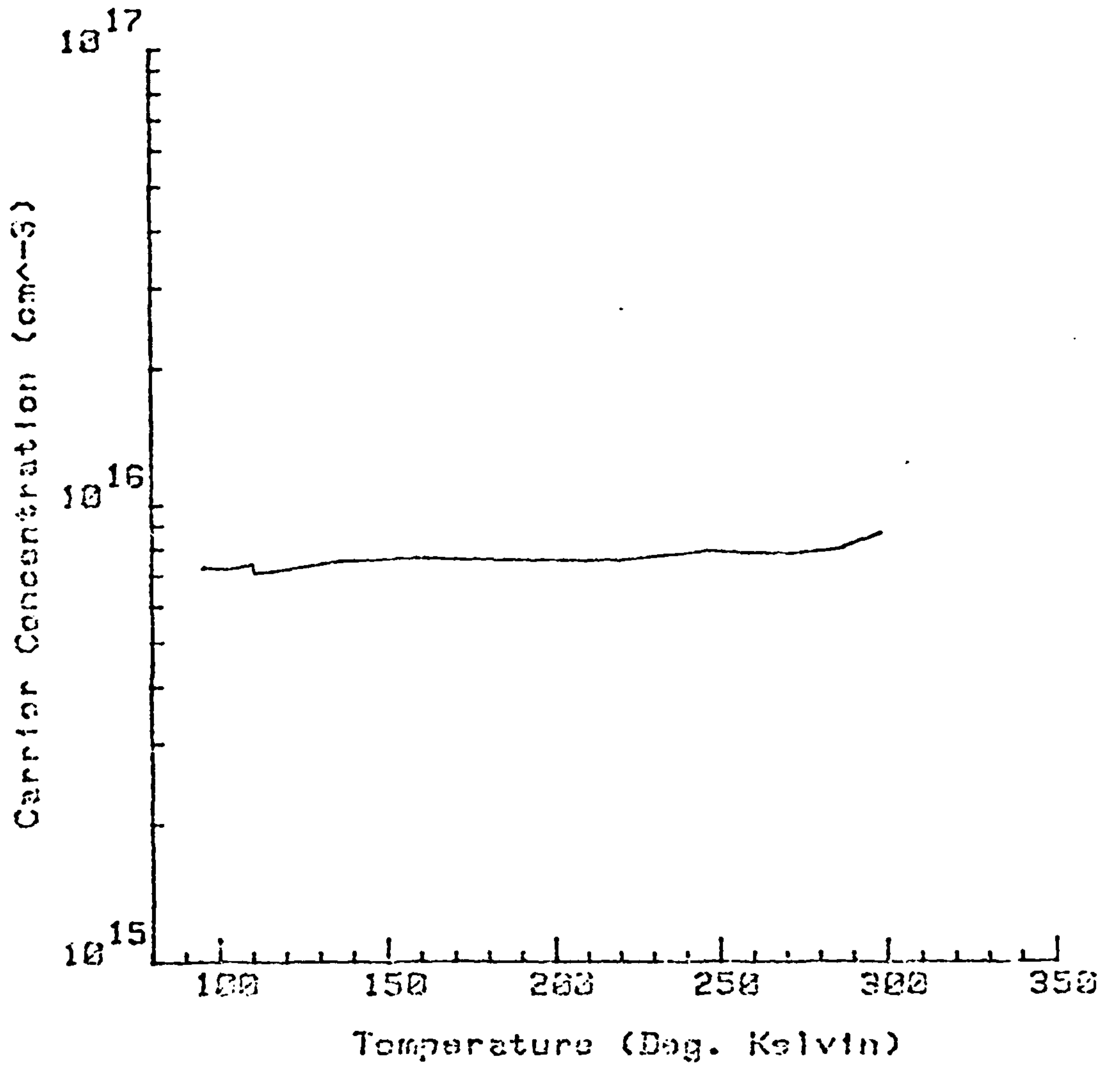

Fig. 3.2 Carrier concentration versus temperature -- GaInAsP sample C1-121.

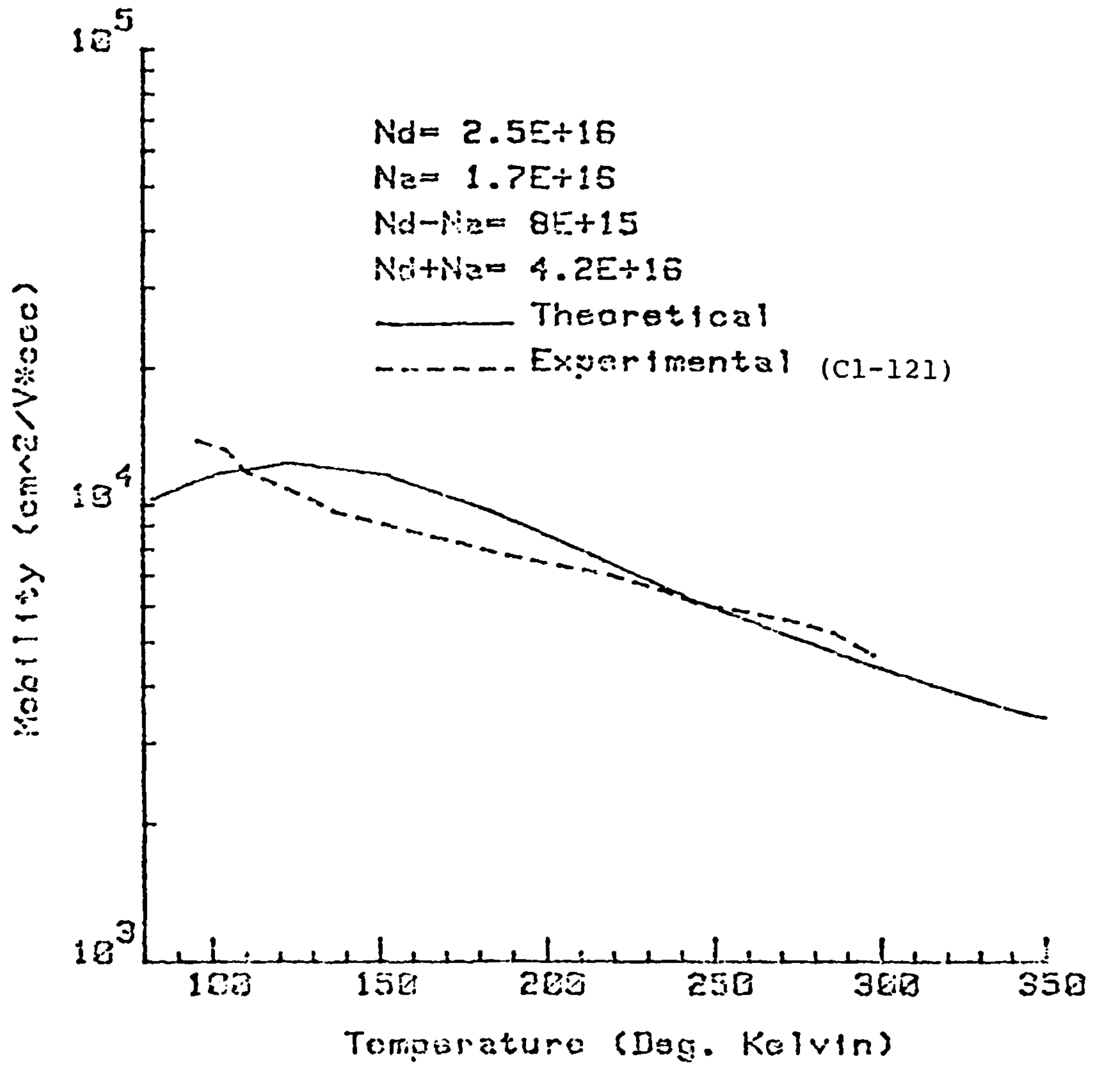

Fig. 3.3 Theoretical fit to experimental mobility versus temperature data: $N_d=2.5\cdot10^{16}$ cm^{-3} and $N_a=1.7\cdot10^{16}$ cm^{-3}.

interpolation techniques. The details of these calculations are described elsewhere [3,4].

A plot of the calculated results for polar optical and acoustic phonon scattering for $x = 0.22$ and $y = 0.46$ is shown in Fig. 3.3. The Brooks-Herring ionized impurity mobility which was used is based on the assumption of Boltzmann statistics which are not strictly valid at low temperatures where the samples are degenerate, but the error introduced should not be major.

The three mobilities: polar optical (μ_{Po}) ; acoustic phonon (μ_{AP}) ; and ionized impurity (μ_{II}) were combined to find the total mobility,

$$\frac{1}{\mu} = \frac{1}{\mu_{Po}} + \frac{1}{\mu_{AP}} + \frac{1}{\mu_{II}} \quad .$$

This is simpler than the more correct calculation involving averaging the sum of the three inverse relaxation times, although, again, the error does not appear to be significant.

A reasonable fit to the particular experimental characteristics shown in Fig. 3.1 is given by the impurity densities $N_D = 2.5 \times 10^{16}\ cm^{-3}$ and $N_A = 1.7 \times 10^{16}\ cm^{-3}$. This is shown in Fig. 3.3 although there is still a significant difference between the experimental and theoretical results at low temperatures. It does appear that the unintentionally doped material that has been grown has a compensation ration N_A/N_D of about 0.7. An even larger compensation ration would be

needed to explain the low mobility values for the material that was used for transferred-electron oscillator studies (see Section 5).

4. HETEROJUNCTION STUDIES

The work involved in this portion of the research program was aimed at determining the electrical characteristics of the n-n heterojunction between GaInAsP and InP. In particular, the conduction band potential energy barrier was a parameter in question. There are extensive derivations in the literature for the expected n-n heterojunction diode current-voltage characteristics for various conduction band lineup conditions. This work is reviewed in a technical report [1].

4.1 Experimental Heterojunction Diodes

The approach used in the experimental work described here was to use the observed current-voltage relations for GaInAsP - InP n-n diodes fabricated as shown in Fig. 4.1. The mesa structures were produced by using the Mesa etch given in Appendix 1. Other details of the diode fabrication are given in the technical report covering this subject [1].

A typical 77° K I-V curve for these diodes is shown in Fig. 4.2. The puzzling aspect of these results is that the polarity for the high-current direction in Fig. 4.2 is opposite to that expected for the anticipated conduction band potential barrier discussed in a technical report [1] and shown here in Fig. 4.3. A plausible explanation of the observed diode characteristics was based on the assumption of low barrier height Schottky barriers at the metal semiconductor contacts

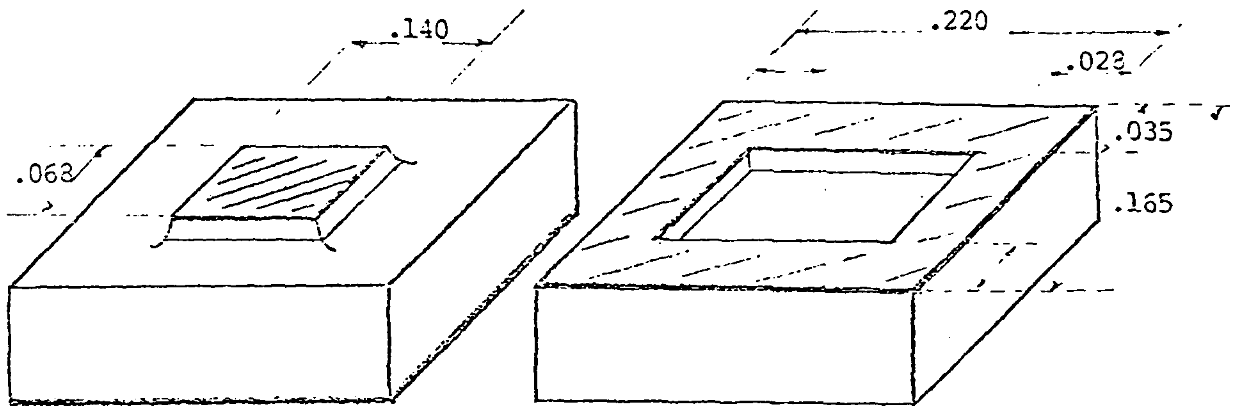

(dimensions in cm)

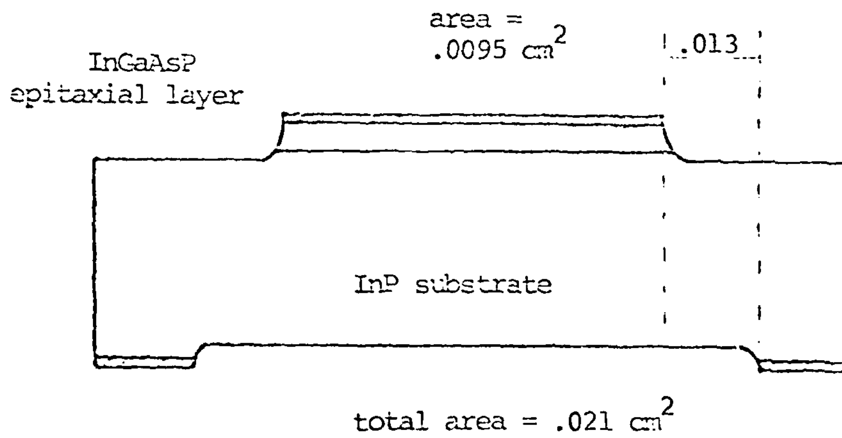

Fig. 4.1 Sketch of Mesa Diode (not to scale)

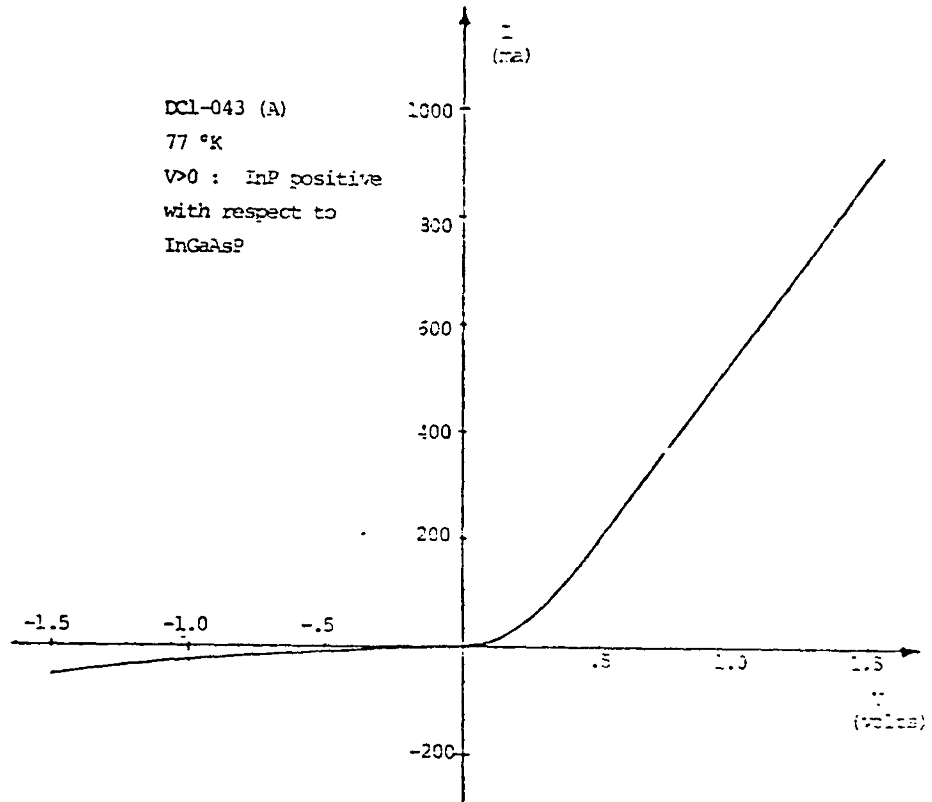

Fig. 4.2 Device I-V Characteristics

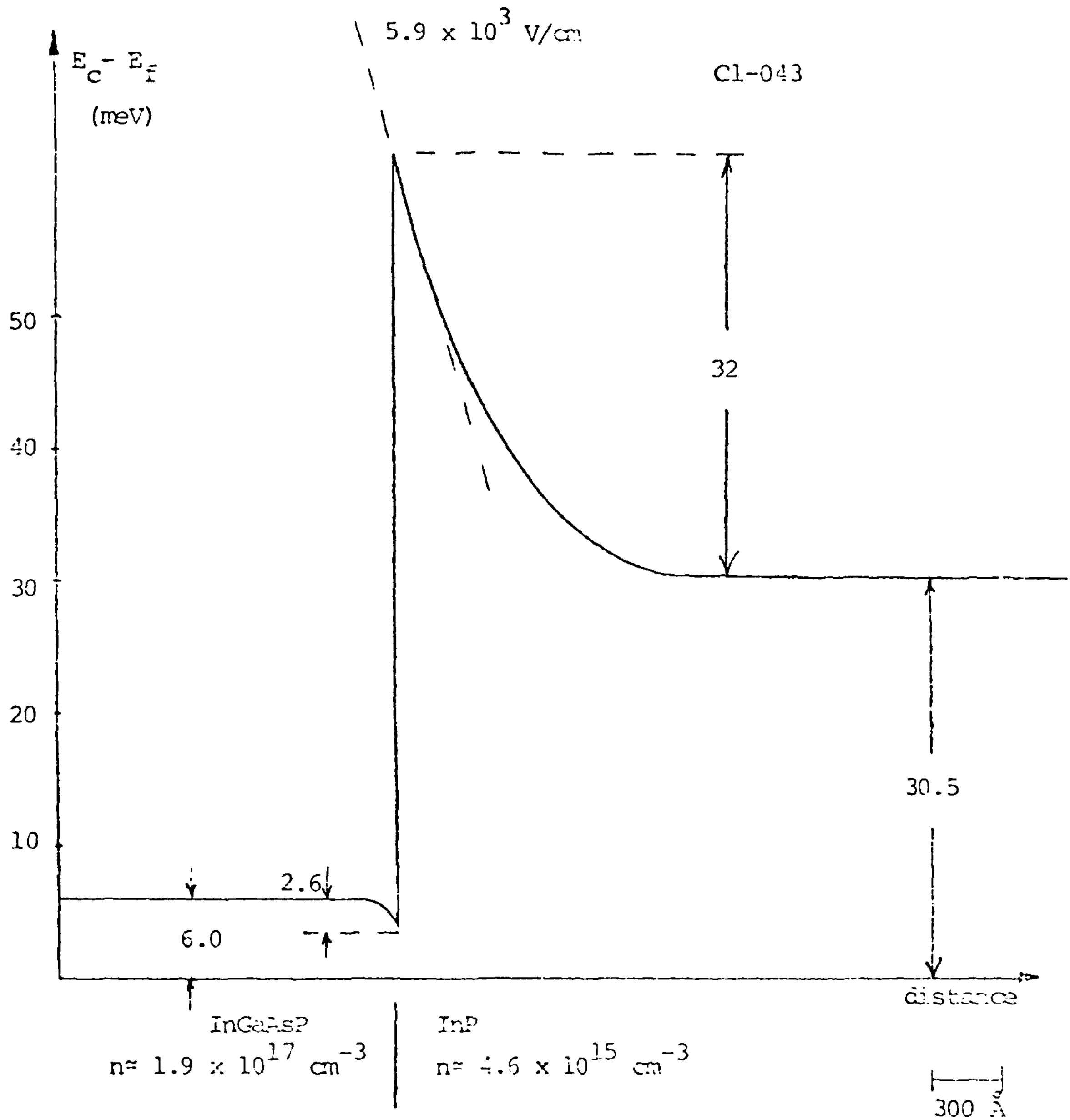

Fig. 4.3 Expected Conduction Band Lineup (Cl-043). The energies are in meV [1].
Quaternary E_g = 1.205 eV, X_{As} = .27, X_{Ga} = .08

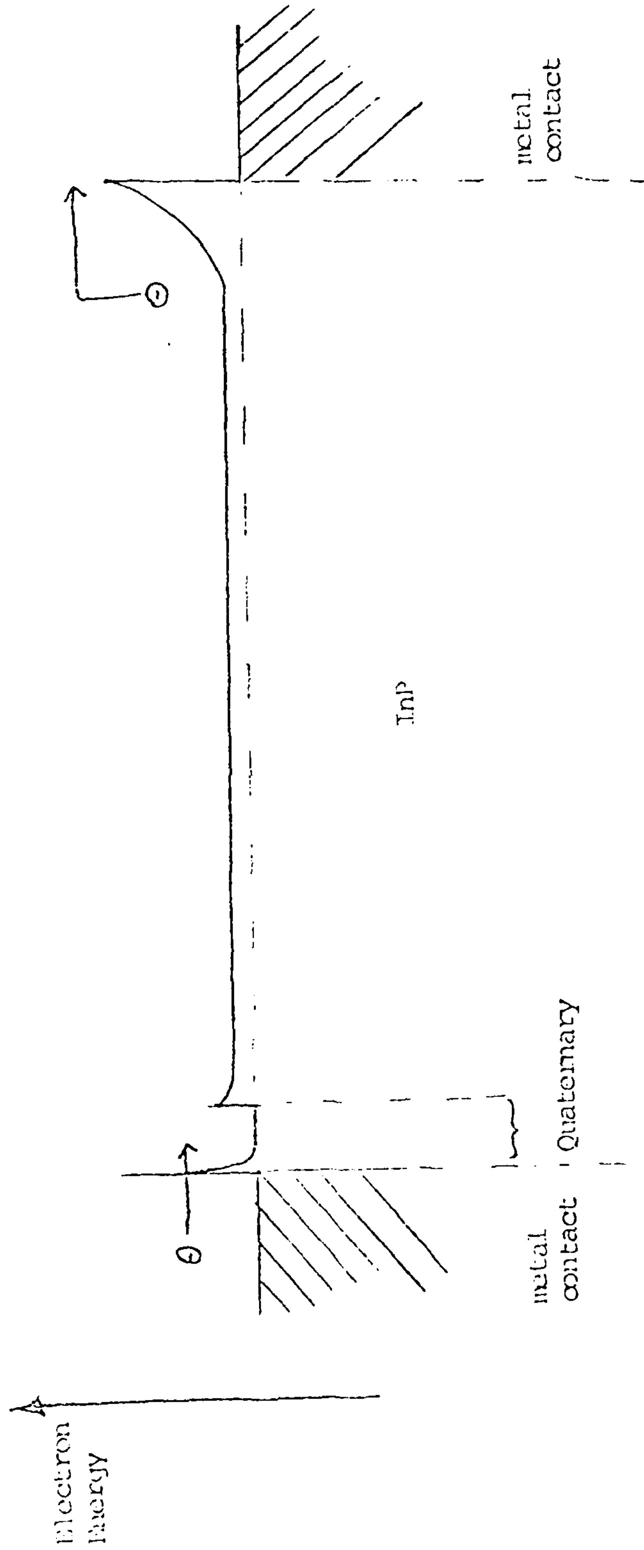

Fig. 4.4 Plausible Device Conduction Band Configuration

used to form the diodes. This band configuration is shown in Fig. 4.4.

4.2 Interpretation of the Data

Assuming that the n-n heterojunction barrier between the quaternary and the InP is small compared to the metal - InP barrier, the device I-V characteristics can be modeled as shown in Fig. 4.5 [1]. Here, the diode represents the metal - InP Schottky barrier and is assumed to fit the equation

$$I_J = I_O[e^{V_J/\eta V_T} - 1] \quad ,$$

where

$$I_O = AeN_D \left(\frac{kT}{2\pi m^*}\right)^{1/2} \exp\left(\frac{-\phi_B}{V_T}\right) \quad .$$

Other definitions are:

- A = diode area
- N_D = donor density
- m^* = electron effective mass
- ϕ_B = semiconductor-to-metal barrier height
- V_T = thermal voltage, kT/e

The experimental results were fit to this device and circuit model for various devices and a summary of the diode parameters are shown in Fig. 4.6. The diode ideality factor, η, is quite large indicating that these experiments do not fit the

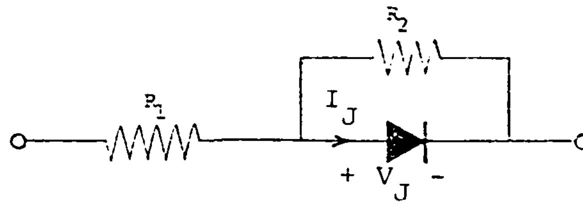

Fig. 4.5 Device Circuit Model

Device	$R_1 (\Omega)$	$R_2 (\Omega)$	I_o (ma)	η	ϕ_B (meV) *
DC1-030(B)	1.5	11.5	5.8	8.0	58
DC1-030(C)	1.5	11.5	7.5	7.3	56
DC1-043(A)	1.3	$\sim\infty$	1.6	7.9	67
DC1-043(B)	2.2	$\sim\infty$	1.1	7.0	69

Fig. 4.6 Summary of Data Analysis

* ϕ_B is the barrier height calculated assuming thermionic emission from the InP substrate to the metal contact. See reference [1] for details.

the expected Schottky barrier physics very well. However, it can be concluded that the quaternary - InP barrier height for electrons is much less than 60 meV for the diodes studied. These results could be explained in terms of grading of the quaternary - InP transition that has been described elsewhere [8]. Such grading can drastically lower the barrier height that might be obtained with an abrupt transition junction.

5. TRANSFERRED ELECTRON EFFECT

In the course of the investigations of the properties of GaInAsP, transferred electroneffect oscillators using this material were studied. This work represents the first observation of the transferred-electron effect in the quaternary. For convenience, the short paper describing this work is reproduced here.

Observation of the transferred-electron effect in $Ga_xIn_{1-x}As_yP_{1-y}$ [a)]

R. E. Hayes and R. M. Raymond

Department of Electrical Engineering, University of Colorado, Boulder, Colorado 80309
(Received 6 May 1977; accepted for publication 14 June 1977)

Transferred-electron oscillation in devices employing $Ga_xIn_{1-x}As_yP_{1-y}$ as the active material has been observed. An oscillation threshold average field of $(5.5-8.6)\times 10^3$ V/cm was determined for 1.05-eV band-gap material having x and y values of approximately 0.13 and 0.37, respectively. A pulsed device had an efficiency of 0.5% at 27.49 GHz.

PACS numbers: 85.30.Fg, 72.20.Ht

It has been pointed out recently that the quaternary semiconductor $Ga_xIn_{1-x}As_yP_{1-y}$ may be of interest for transferred-electron device applications because of the electron-velocity—electric-field relation that is calculated for this material.[1] The purpose of this paper is to give some experimental characteristics of a $Ga_xIn_{1-x}As_yP_{1-y}$ transferred-electron oscillator. We believe this to be the first report of the observation of transferred-electron oscillation in this material, although velocity-field data suggesting the onset of electron transfer have been reported.[2]

The quaternary material used in the experiments reported here was grown by standard liquid-phase epitaxy techniques on an InP substrate.[3,4] The substrate growth surface was within 0.7° of the (100) orientation and was Sn doped with a net electron concentration of 1.0×10^{18} cm^{-3}. The $Ga_xIn_{1-x}As_yP_{1-y}$ layer was grown by the ramp cooling technique over the temperature range 650–630 °C. The epitaxial layer was not intentionally doped, but was observed to be n type, as is typical of our quaternary layers. The electron density and mobility of the transferred-electron devices described below were determined from the low-field resistance and the geometrical transverse magnetoresistance effect.[5] The results for the device reported were $n = 1.0\times 10^{15}$ cm^{-3} and $\mu = 2630$ cm^2 V^{-1} sec^{-1}. It should be noted that this mobility is much lower than the value expected for an ionized donor density of $1.0\times 10^{1?}$ cm^{-3},[1,4] indicating that the density of scattering centers is considerably greater than that value.

The thickness of the epitaxial layer was 4.5 ± 1.0 μ as determined by optical examination of a cleaved and etched surface. The 75 °K energy band gap and 300 °K lattice constant of the grown layer, as determined by photoluminescence and x-ray diffraction techniques, were 1.10 eV and 5.885 Å, respectively. This energy gap corresponds to about 1.05 eV at 300 °K. The quaternary layer lattice constant is not quite matched to that of InP. The composition was estimated by using a modified form of the relations that have been devel-

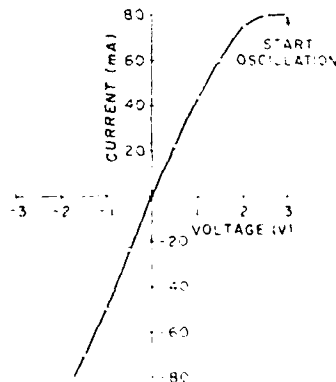

FIG. 1. The current-voltage characteristic for the transferred-electron oscillator described in the text. The voltage shown is that of the substrate with respect to the epitaxial layer contact.

[a)] The work reported was supported by the Office of Naval Research.

Copyright © 1977 American Institute of Physics

oped for the band gap and lattice constant as a function of the composition parameters.[5,6] The results for the layer reported here are $x = 0.13$ and $y = 0.37$.

Ohmic contacts for the devices were produced on both the substrate and active-layer sides by evaporation of Sn and then Ag (500 and 5000 Å, respectively) and subsequent alloying in forming gas at 450 °C for 60 sec. The device areas were then formed by photoresist techniques and etching. The final devices consisted of circular mesas 75 μ in diameter and 11 μ high on a 380-μ square die. The devices were mounted mesa up in a package consisting of a metal stud with two metallized quartz cube stand-offs (500 μ on an edge) that provided bonding pads for the 25-μ-diam Au wire used to connect to the mesa contact. All bonding was by low-temperature soldering techniques.

The packaged devices were tested in the center of a reduced-height *Ka*-band waveguide mount having provisions for applying a bias. The mounting section tapered into standard height guide, and a sliding short and an *E-H* tuner were used to define the oscillator cavity. The bias consisted of voltage pulses 0.4 μsec long, and the microwave power was detected by means of a calibrated crystal detector.

The current-voltage curve for one device is shown in Fig. 1. It is evident that the contacts are essentially Ohmic, although there is a slight evidence of device asymmetry. The observed start-oscillation point of 3.0 V yields, using an active-layer thickness of 4.5 ± 1.0 μ, an average field of $(5.5-8.6)\times 10^3$ V/cm. These values are larger than the 5×10^3 V/cm predicted by Littlejohn *et al.* for a quarternary having approximately the same band gap as here (although exactly lattice matched).[1] This higher threshold field is consistent with the low mobility of the material used in these experiments. Also, experimental start-oscillation average field values are circuit dependent and may certainly overestimate the true peak-velocity field for the material.

The oscillation characteristics were observed at a bias voltage of 5.5 V and a current of 70 mA. The peak pulse output power at 27.49 GHz was 2.0 mW, and the efficiency was 0.5%. No attempt was made, in these experiments, to optimize the circuit, bias, or frequency for this particular device.

In summary the results presented show that *n*-type $Ga_xIn_{1-x}As_yP_{1-y}$, grown on InP by liquid-phase epitaxy, can be used for transferred-electron oscillators. The average oscillation threshold field observed in material having a 300 °K band gap of 1.05 eV is in the range $(5.5-8.6)\times 10^3$ V/cm, which is somewhat higher than theoretical predictions for the peak-velocity field. The evaluation of the potential importance of this quaternary material for transferred-electron device applications requires a more extensive material and device investigation than presented here.

[1]M.A. Littlejohn, J.R. Hauser, and T.H. Glisson, Appl. Phys. Lett. 30, 242 (1977).

[2]B.B. Houston, J.B. Restorff, J.R. Burke, and R.E. Hayes, APS Solid State Meeting, San Diego. 1977, Paper CK10 (unpublished).

[3]G.A. Antypas and R.L. Moon, J. Electrochem. Soc. 120, 1574 (1973).

[4]R. Sankaran, G.A. Antypas, R.L. Moon, J.S. Escher, and L.W. James, J. Vac. Sci. Technol. 13, 932 (1976).

[5]T.R. Jervis and E.F. Johnson, Solid-State Electron. 13, 181 (1970).

[6]R.L. Moon, G.A. Antypas, and L.W. James, J. Electron. Mater. 3, 635 (1974).

6. ANODIC OXIDES

This work had as its goal the investigation of the characteristics of anodic oxides grown on the n-type quaternary. The quaternary epitaxial layers were anodically oxidized using an experimental set-up such as is shown in Fig. 6.1. In various cases constant voltage or constant current anodization was used with little difference in the oxides produced. The properties of anodic oxide layers on InP were also studied in order to provide a comparison with the quaternary results. Details of oxidation techniques and interpretation of the experimental metal-oxide-semiconductor capacitance results that were used to determine the oxide characteristics are given in the technical reports covering this topic [9,10].

6.1 MOS Measurements

The anodization used to make MOS capacitors employed an electrolyte consisting of 1 part of 3% tartaric acid in water adjusted to a pH of 6 using NH_4OH mixed with 3 parts of ethylene glycol [11]. A typical anodization current vs time relation for a quaternary sample (C1-068 here having $x_{In} = 0.85$ $y_{As} = .15$) is shown in Fig. 6.2. This epitaxial layer, having $n = 7 \times 10^{16}$ cm^{-3} was anodized for 10 minutes.

Al dots 10^{-2} inch in diameter were evaporated on the oxide and evaporated Sn ohmic contacts were formed on the n^+ InP substrate. Metal-Oxide-Semiconductor (MOS) capacitance voltage measurements were made to determine the oxide-

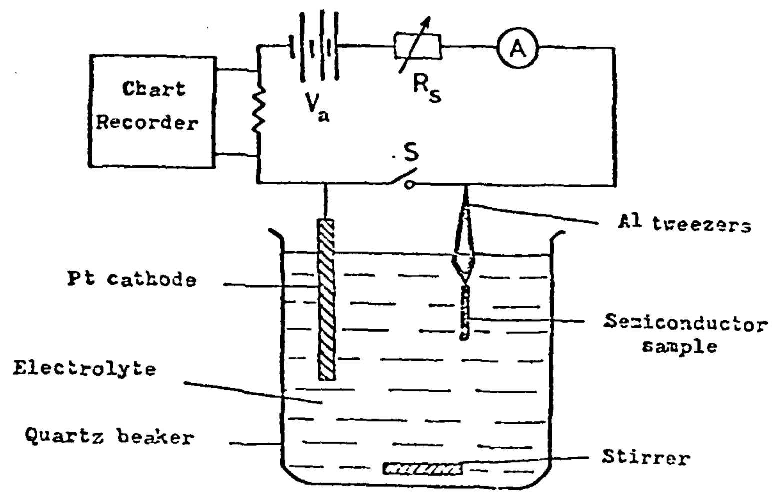

Fig. 6.1 Experimental setup for anodic oxidation of semiconductor.

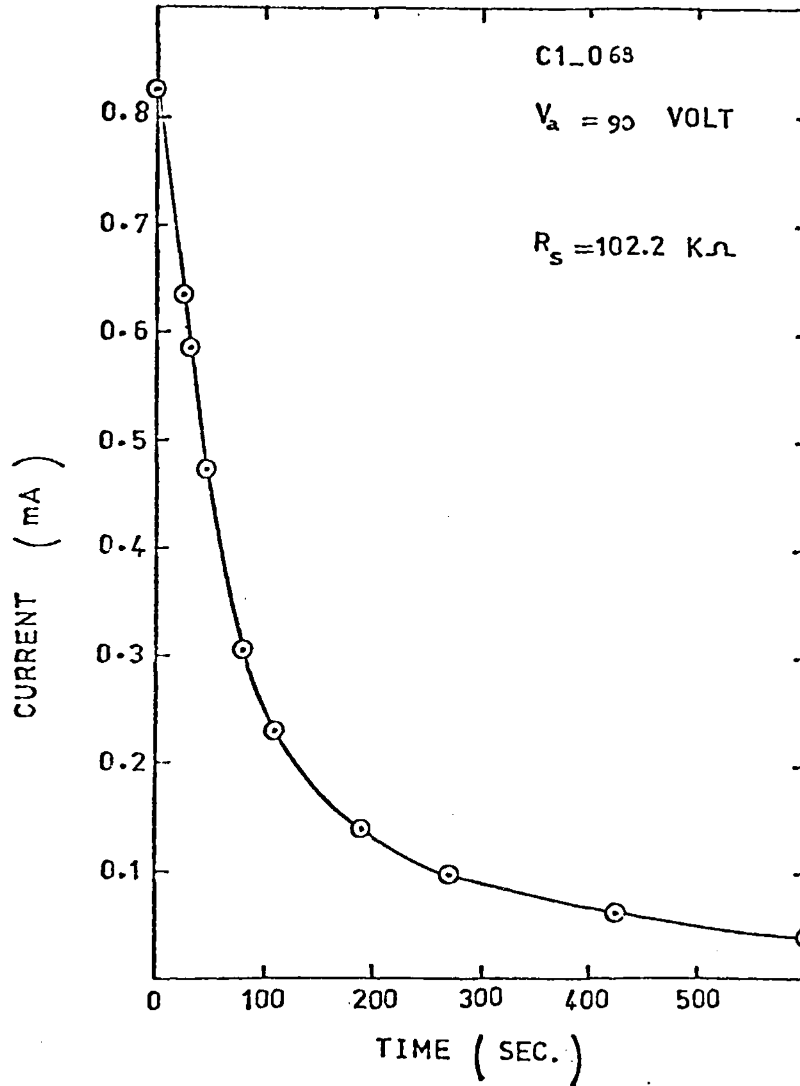

Fig. 6.2 Anodization current behavior for GaInAsP (sample area = 0.5 cm^2).

semiconductor interface properties. Typical results are shown in Fig. 6.3. The oxide was determined to be 1150 A° thick by optical interference measurements and the oxide relative dielectric constant was found to be about 6.5 from the positive voltage saturated capacitance.

The C-V measurements shown in Fig. 6.3 were used to determine the surface state density as a function of the surface potential. (The surface potential was taken to be zero at the conduction band edge and negative for energies below the band edge.) Typical surface state densities are shown in Fig. 6.4.

In addition to the surface state density, other parameters measured included the oxide dielectric constant, the oxide resistivity and breakdown field. A summary of these results and comparison with other anodic oxide results are shown in Tables 6.1 through 6.4.

6.2 Surface-State Time Constants

The frequency dependence of the capacitance-voltage measurements for the MOS structures was used to determine the time constant of the quaternary surface states [18]. The equivalent circuit assumed for this work is that shown in Fig. 6.5 [18]. The surface state time constant, τ, ($\tau = R_S C_S$, see Fig. 6.5) was calculated by fitting the observed capacitance-voltage relations over a frequency range of 20 Hz to 1 mHz, as shown in Fig. 6.6 to the equivalent circuit shown in Fig. 6.5. The resulting surface-state time

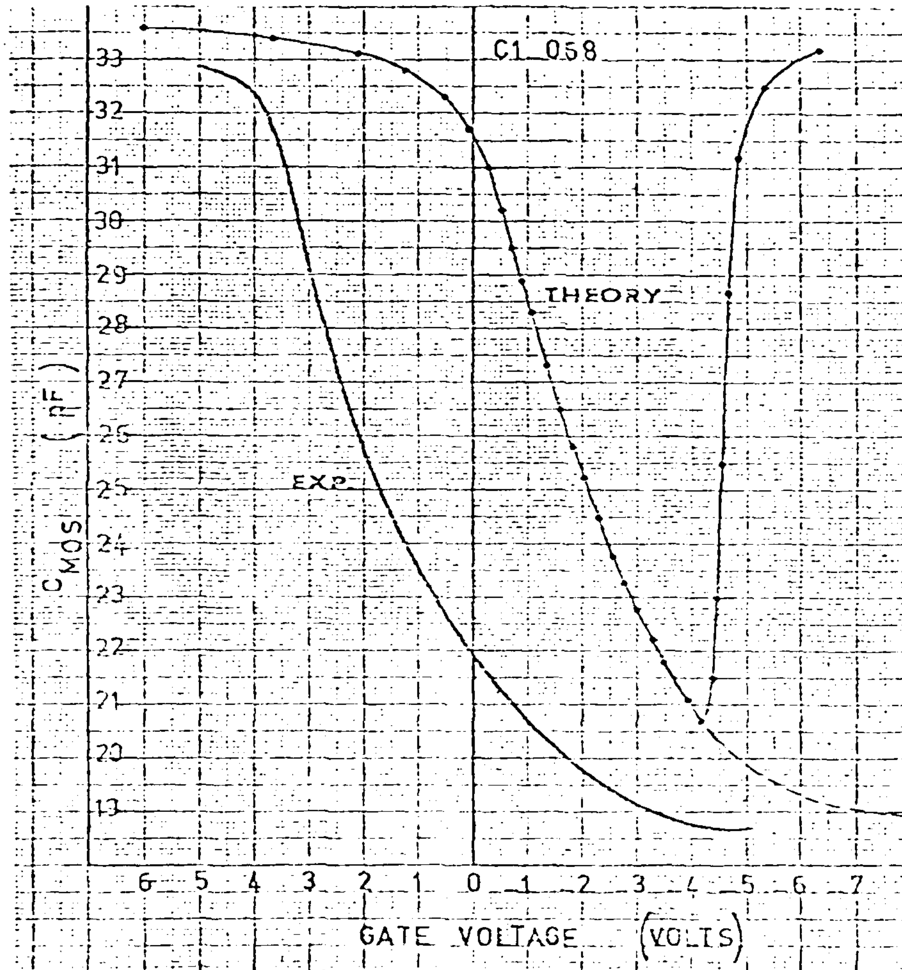

Fig. 6.3 Ideal C-V characteristic for a MOS diode fabricated on GaInAsP compared to the experimental one (T_{ox} = 1150 Å).

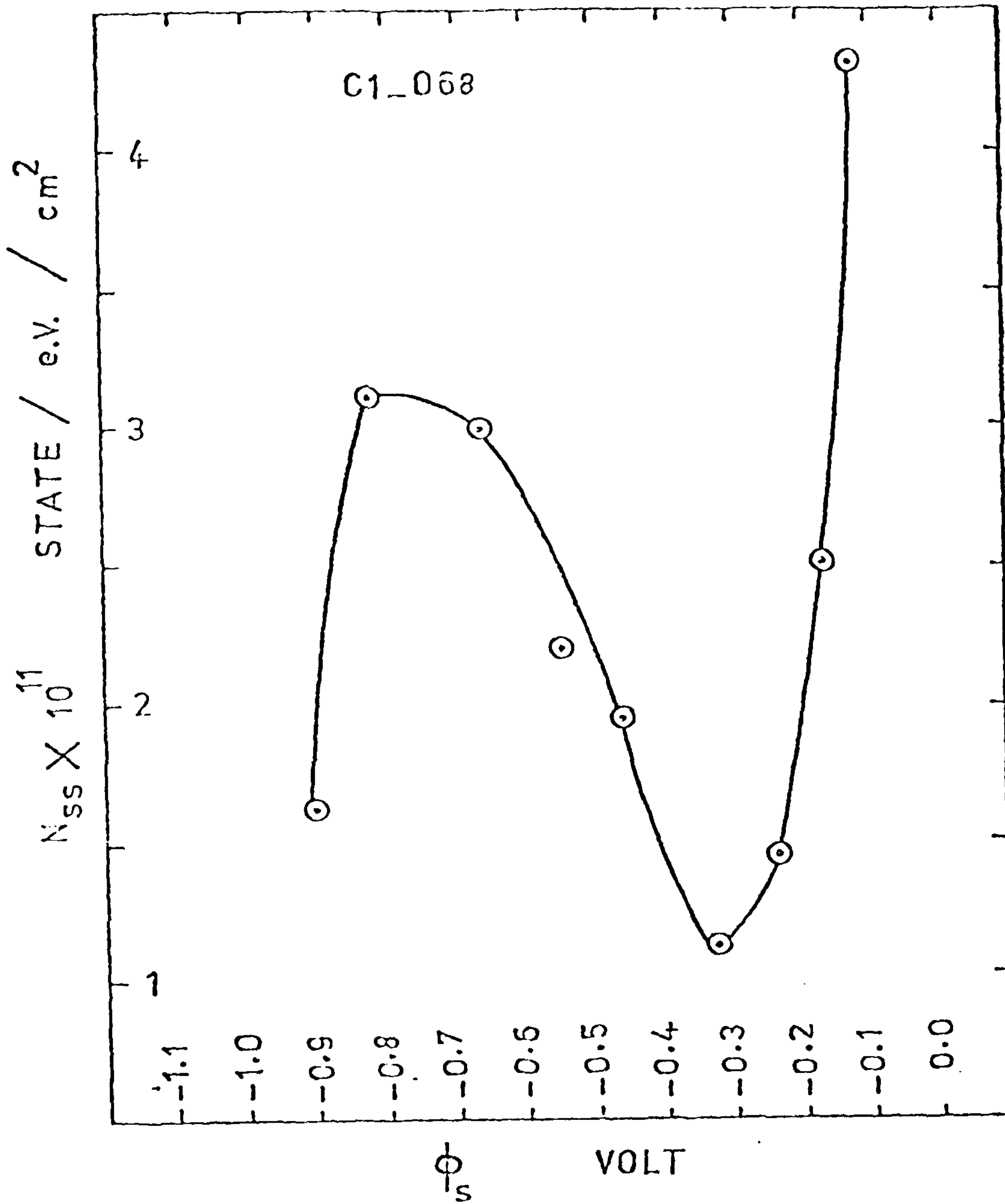

Fig. 6.4 Surface State Density against the Surface Potential for a MOS device fabricated on GaInAsP.

TABLE 6.1

DIELECTRIC CONSTANT OF OXIDES GROWN ANODICALLY ON InP AND GaInAsP AND OTHER MATERIALS

Material	Electrolyte	ε_{ox} (at 1 MHz)	Reference
InP	Glycol and water	4.3	This work [9]
GaInAsP*	Glycol and water	6.5	This work [9]
InP	1% by weight solution of sodium salicylate in ethyl alcohol	4.4	[12]
GaAs	Glycol and water	7-8	[11]
GaP	H_2O_2 30 % - pH ≈ 2	5.7	[13]
InSb	0.1 N solution of KOH	11-12	[14]
Si	0.04 mole KNO_3 in N-methylacetamide	3.8	[15]

* $Ga_xIn_{1-x}As_yP_{1-y}$ with x = 0.15, y = 0.15, Eg = 1.266 e.V. at 77°K.

TABLE 6.2

OXIDE SPECIFIC RESISTANCE FOR InP AND GaInAsP AND OTHER MATERIALS

Material	Electrolyte	ρ (ohm-cm)	Reference
InP	Glycol and water	4.4×10^{10}	This work [9]
GaInAsP*	Glycol and water	1.2×10^{10}	This work [9]
InP	Glycol and water	10^{10} - 10^{11}	[11]
GaAs	Glycol and water	10^{14} - 10^{16}	[16]
GaP	H_2O_2 30% - pH ≈ 2	10^{14}	[13]
Si	0.04 mole KNO_3 in N-methylacetamide	10^{12} - 10^{16}	[15]

* $Ga_xIn_{1-x}As_yP_{1-y}$ with x = 0.5, y = 0.38, Eg = 1.11 e.V. at 77°K, a = 5.876°A at 300°K.

TABLE 6.3

OXIDE BREAKDOWN FIELD FOR InP AND GaInAsP AND OTHER MATERIALS

Material	Electrolyte	Oxide Breakdown Field (V/cm)	Reference
InP	Glycol and water	4×10^6	This work [9]
GaInAsP*	Glycol and water	$1\text{-}2 \times 10^6$	This work [9]
InP	Glycol and water	$2\text{-}3 \times 10^6$	[11]
GaAs	Glycol and water	$4\text{-}5 \times 10^6$	[11]
GaP	H_2O_2 30% - pH = 2	6×10^6	[13]

* $Ga_xIn_{1-x}As_yP_{1-y}$ with x = 0.15, y = 0.38, Eg = 1.11 E.V. at 77°K, a = 5.876 °A at 300°K.

TABLE 6.4

INTERFACE STATE DENSITY IN CASE OF
InP and GaInAsP AND OTHER MATERIALS

Material	Electrolyte	N_{ss} (state/e.V./cm^2)	Reference
InP	Glycol and water	1-4 x 10^{11}	This work [9]
GaInAsP*	Glycol and water	2-3 x 10^{11}	This work [9]
InP	1% by weight solution of sodium salicylate in ethyl alcohol	3-4 x 10^{11}	[12]
GaAs	mixture of water and tartaric acid and polyhydric	1-2 x 10^{11}	[17]

* $Ga_xIn_{1-x}As_yP_{1-y}$ with x = 0.15, y - 0.15, Eg = 1.266 e.V. at 77°K.

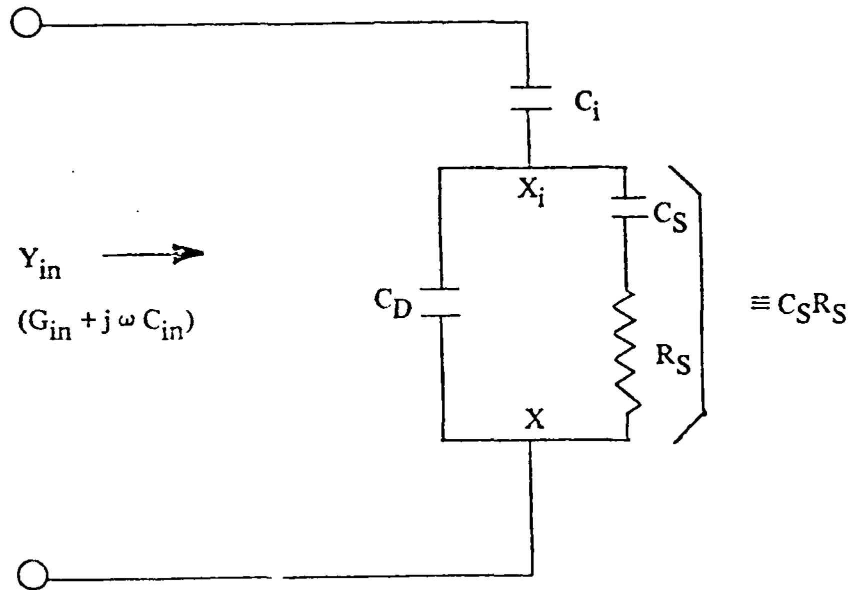

Fig. 6.5 Equivalent circuit including surface states affect where C_S and R_S are associated with surface states densities.

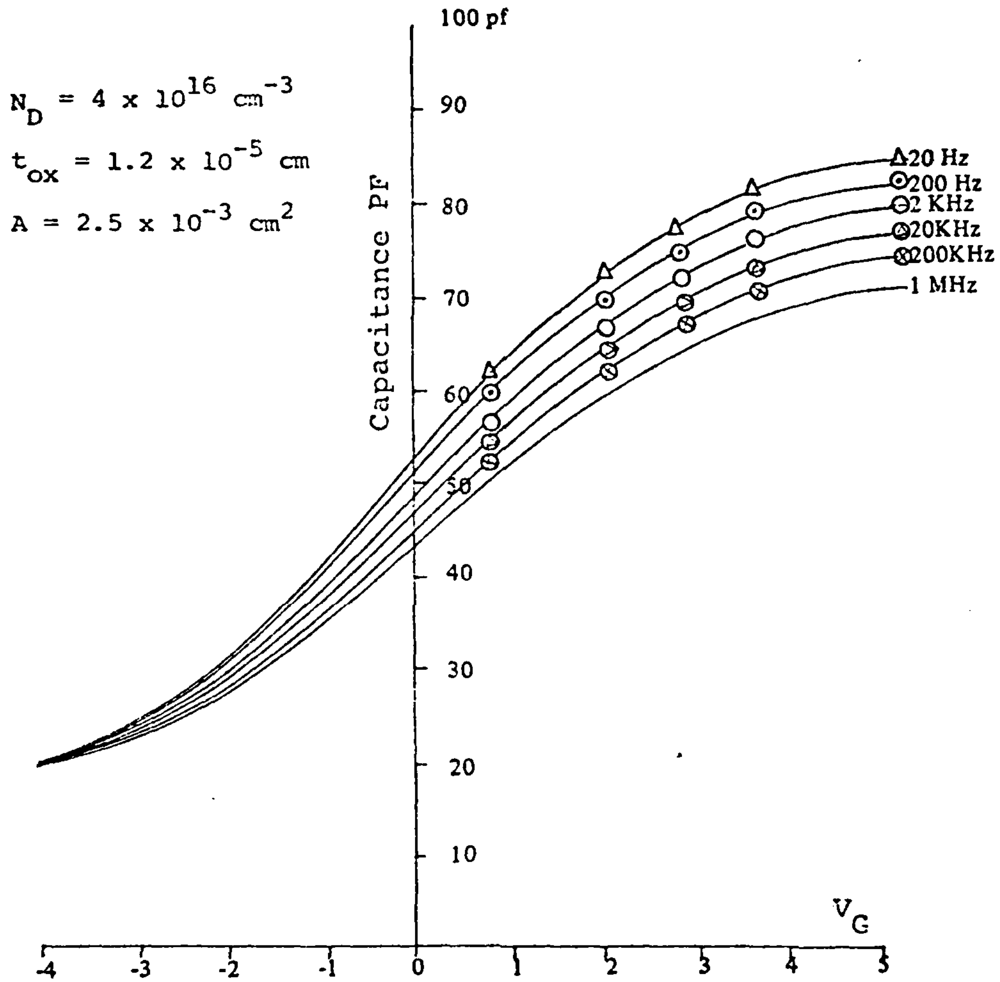

Fig. 6.6 C-V curves with a frequency as a parameter for $In_xGa_{1-x}As_yP_{1-y}$. Data points for $V_G < 0$ are not shown in order to avoid crowding (x = 0.79, y = 0.45).

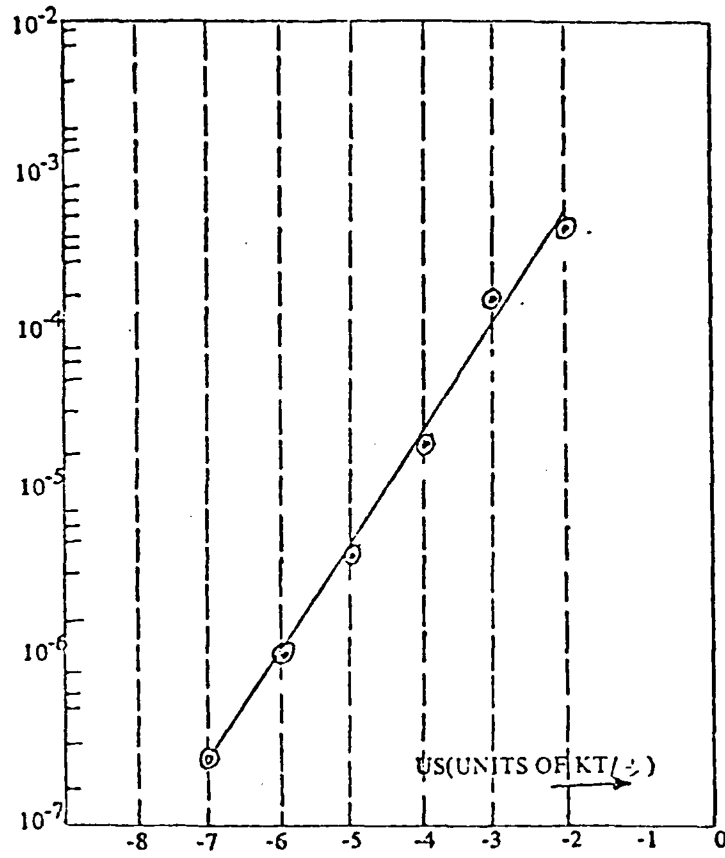

Fig. 6.7 Surface state time constant as a function of surface potential $In_xGa_{1-x}As_yP_{1-y}$ (Cl-104) having:

$N_D = 7 \times 10^{16}\ cm^{-3}$ $x = 0.79$

$t_{ox} = 1.15 \times 10^{-5}\ cm$ $y = 0.45$

$A = 6.7 \times 10^{-4}\ cm^2$

constant for quaternary layer Cl-104 are shown in Fig. 6.7. The magnitude of these time constants are very similar to values obtained in our laboratory for anodic oxides on n-type InP.

7. CONCLUSION

Conditions for the growth by liquid phase epitaxy of quaternary semiconductor $Ga_xIn_{1-x}As_yP_{1-y}$ layers on (100) InP substrates were established and properties of this material and devices employing the quaternary were investigated. The best epitaxial layers were of high quality having mirror-like surfaces and compositional and electrical homogeneity.

It was found that, for the material investigated, the experimental electron mobility results could be explained with a theory that did not include an alloy scattering contribution. However, purer material (that studied here generally had about 10^{16} cm^{-3} carriers) would be necessary to accurately assess the role of alloy scattering in the quaternary.

Studies of isotype heterojunction diodes of GaInAsP - InP indicated that the conduction band discontinuity is less than about 60 meV. It appears likely that these results may have been influenced by grading of the heterojunction during growth and a more accurate evaluation will require growth techniques that produce very abrupt heterojunction transitions.

The first observations of transferred electron (TE) oscillators were made during these investigations. The results tend to support the theoretical predictions that the quaternary would be a superior material for TE oscillators in the millimeter wavelength range. However, it does appear that the advantage that the quaternary may have over InP is small and that InP will most likely remain the preferred material for microwave

and millimeter wavelength devices.

Anodic oxides on the quaternary were investigated by MOS capacitor techniques. The observed surface state densities were similar to those that have been observed on other III-V materials. However, the oxide resistivity for the quaternary, and for InP, was much lower than the values that have been reported for GaAs. These results suggest that the insulator for MIS devices using GaInAsP (and InP) should not be produced by anodic oxidation.

REFERENCES

1. S.C. Wright, "Growth and Characterization of $In_xGa_{1-x}As_yP_{1-y}$-InP n-n Heterojunctions", Solid State Electronics Report 78-5-1, Electrical Engineering Department, University of Colorado.

2. R.E. Hayes, "Tables of the Compositional Dependence of the Energy Bandgap and Lattice Constant for $Ga_xIn_{1-x}As_yP_{1-y}$", Solid State Electronics Report 77-6-1, Electrical Engineering Department, University of Colorado.

3. E. Marchand, "An Electrical Evaluation of $Ga_xIa_{1-x}As_yP_{1-y}$", Solid State Electronics Report 79-6-1, Electrical Engineering Department, University of Colorado.

4. C.D. Forgerson, "Mobility and Carrier Concentration in GaAs and GaInAsP", Solid State Electronics Report 81-3-1, Electrical Engineering Department, University of Colorado.

5. J.W. Harrison and J.R. Hauser, "Theoretical Calculations of Electron Mobility in Ternary III-V Coumpounds", J. of Applied Physics, Vol. 47, No. 1, 1976, pp 292-300.

6. M.A. Littlejohn, J.R. Hauser, T.H. Glission, D.K. Ferry, and J.W. Harrison, "Alloy Scattering and High Field Transport in Ternary and Quaternary III-V Semiconductors", Solid State Electronics, Vol. 21, 1978, pp 107-114.

7. B.R. Nag, Theory of Electrical Transport in Semiconductors, Pergamon Press, N.Y., 1972, p. 105.

8. R.M. Raymond and R.E. Hayes, "Barrier Light Reduction for Graded n-n Heterojunctions", J. Appl Phys, Vol. 48, No. 3, March 1977, pp 1359-60.

9. A.A.R. Elshabini, "Characteristics of Anodic Oxide Films on InP and GaInAsP", Solid State Electronics Report 78-5-2, Electrical Engineering Department, University of Colorado.

10. M.M. El-Muradi, "A Study of Surface State Parameters and an Investigation of the Surface Charge Behavior with Charging Frequency for InP and $In_xGa_{1-x}As_yP_{1-y}$ Materials", Solid State Electronics Report 79-4-1, Electrical Engineering Department, University of Colorado.

11. H.L. Hartnagel, "MOS Gate Technology on GaAs and other III-V Compounds", J. Vac. Sci. Technol., Vol. 13, No. 4, July/Aug. 1976.

12. D.L. Lile and D.A. Collins, "An InP MIS Diode", Appl. Lett., Vol. 28, No. 9, May 1976, pp 554-556.

13. T. Ikoma and H. Yokomizo, "C-V Characteristics of GaP MOS Diode with Anodic Oxide Film", IEEE Trans. on Electron Devices, Vol. 23, May 1967, p 521.

14. R.K. Mueller and R.L. Jacobson, "Photocontrolled Surface in Anodized InSb", J. Appl. Phys., Vol. 35, No. 5, May 1964, pp 1524-1529.

15. P.F. Kane and G.B. Larrabee, "Characterization of Semiconductor Materials", Texas Instr. Electr. Series, McGraw-Hill Book Company, 1970.

16. R.A. Logan, B. Schwartz and W.J. Sundburg, "The Anodic Oxidation of GaAs in Aqueous H_2O_2 Solution", J. Electrochem. Soc., Solid State Science and Technology, Vol. 120, No. 10, Oct. 1973, pp 1385-1390.

17. Hideki Hasegawa, K.E. Forward and H.L. Hartnagel, "New Anodic Native Oxide of GaAs with Improved Dielectric and Interface Properties", Appl. Phys. Lett., Vol. 26, No. 10, May 1975.

18. Deuling, E. Klausmann, and A. Goetzberger, "Interface State in Si-SiO_2 Interfaces", Solid State Electronics, Vol. 15, 1973, pp 559-571.

APPENDIX 1

Substrate Preparation and InP Etching and Processing Techniques

InP Substrate Processing

Growth Wafers

1. Slices from original ingot (approximately 22 mils thick) are mounted on talc block using black wax.
2. Wafers approximately 1/2 × 1 cm are cut from the slice.
3. Wafers are de-mounted from talc block, then mounted on cylindrical slugs for polishing; using TCE and heat where appropriate.
4. Mechanical hand polishing on glass plate using alumina (~3.0μ) abrasive and H_2O . Approximately 5.5 mils of material removed.
5. Mechanical polishing on PAN-W pads, using alumina abrasive, soap and H_2O. First 1.0μ abrasive is used, removing approximately 0.3 mils of material, then 0.3μ, removing 0.1 mils, then 0.05μ , removing 0.1 mils.
6. Wafers are then de-mounted, turned over on their holders and steps 4 and 5 are repeated.
7. Chemical-mechanical polishing on PAN-W pad, using 0.3% solution of Br-Meth. Enough material is removed (approximately 0.4 mils) to achieve the desired thickness (around 9.6 - 9.7 mils).
8. Substrates are then de-mounted using TCE and heat, and placed into a solvent extractor. The following chemicals are given at least 10 flushes (in the order given):

TCE

acetone

isopropyl alcohol

methyl alcohol

9. Finally the substrates are etched 15 sec. in $H_2SO_4:H_2O_2:H_2O$ (5:1:1), flushed in distilled H_2O; then etched approximately 20 sec. on 0.3% Br-Methanol rinsed in Methanol and blown dry with N_2 gas.

Saturation Wafers

1. Slices are cut from original polycrystalline ingot approximately 20 mils thick.
2. The slice is then mounted on a talc block and cut into wafers approximately 0.5 × 1.0 cm.
3. Wafers are then mounted on cylindrical slugs for polishing.
4. Mechanical hand polishing on glass plate using alumina 3.0μ abrasive and H_2O. Approximately 5 mils removed.
5. Wafers are then turned over and step 4 is repeated until the desired thickness (approximately 11 mils) is obtained.
6. Wafers are then de-mounted and placed in the solvent extractor and the same procedure as for growth wafers is followed.
7. Etching -- same as for growth wafers.

Some InP Etching and Processing Techniques

Br_2-Methanol

2.0% Br_2 by vol. etches (100) surfaces at approximately 1μ/min.

0.3% Br_2 by vol. slower etching rate than above.

We get variable results with this etch as far as the enhancement of surface damage is concerned.

5:1:1 Etch

$H_2SO_4:H_2O_2:H_2O$ in 5:1:1 ratio by volume

Removes approximately 1000 Å in 5 min. at room temperature on (100) surfaces.

$Br_2:HBr:H_2O$ (Mesa Etch)

Use 1:17:35 by volume at room temperature. Removes 22 microns per minute on (100) surfaces. Produces good mesas with photoresist.

A-B Etch (delineation of interfaces)

Solution A: 40 cc H_2O + 0.3 g $AgNO_3$ + 40 cc HF

Solution B: 40 cc H_2O + 40 g CrO_3

Prepare solutions and keep indefinitely.

Mix equal parts of A and B and place cleaved face in solution for several seconds at room temperature. Rinse with H_2O, repeat if necessary to clearly delineate interface. Works well on GaInAsP-InP interfaces. (General reference: Olsen & Ettenberg, J. of Appl. Phys., v.45, pp. 5112-5114, Nov. 1974).

Melt Removal

Mix: N-N dimethylformamide (50ml) and mercuric chloride (10.6 g). Use 5-10 ml in ultrasonic bath for approximately one minute to remove melt. Solution keeps well.

DATE
FILMED
8